Associations between neutral and ionized gas in SGR A

Liszt, H.S.; Burton, W.B.; Hulst, J.M. van der

Astron. Astrophys. 142, 237–244 (1985)

ASTRONOMY AND ASTROPHYSICS

Associations between neutral and ionized gas in Sgr A

H.S. Liszt [1], W.B. Burton [2], and J.M. van der Hulst [3]

[1] National Radio Astronomy Observatory, Edgemont Road, Charlottesville, VA 22901, USA
[2] Sterrewacht Leiden, Postbus 9513, NL-2300 RA Leiden, The Netherlands
[3] Netherlands Foundation for Radio Astronomy, Radiosterrewacht Westerbork, Schattenberg 4, NL-9433 TA Zwiggelte, The Netherlands

Received March 22, accepted July 9, 1984

Summary. We consider the morphology of the radio continuum radiation from Sgr A and that of several kinematic components of the neutral molecular and atomic gas, most notably the 50 km s^{-1} cloud. The large-scale (15 arcmin or $\simeq$ 50 pc) radio and infrared continuum structure follows closely the *borders* of the 50 km s^{-1} cloud: correspondence between the radio arc feature and the boundary of the cloud suggests that the shape of the arc is determined by the neutral material. At the other end of the cloud, the source Sgr A lies just outside the boundary of the neutral material, but a strong emission peak in CO is coincident with a newly-discovered cluster of H II regions.

On a smaller scale, we show that Sgr A* and Sgr A (West) are encircled by a ring of gas, visible in H I and ^{12}CO, with radius $\simeq$ 3 pc and rotation velocity $\simeq$ 110 km s^{-1}; the smaller double-lobed structure seen at long infrared wavelengths represents the heated inner edge of this neutral gas distribution. It is this ring, not the 50 km s^{-1} cloud, which provides 40–60 km s^{-1} H I or H_2CO absorption toward Sgr A (West). The ring has a peculiar orientation with respect to the galactic equator but this geometry is also seen in the radio and infrared continuum radiation, and in the kinematics of ^{12}CO, over some 50 pc near Sgr A.

Key words: galactic center – H I regions – interstellar clouds – molecular clouds – interstellar absorption

1. The large-scale morphology of the Sgr A complex

1.1. The radio continuum

The radio continuum structure of the Sgr A complex was first elucidated by Downes and Maxwell (1966). Immersed in a weaker, diffuse background are Sgr A itself at $(l, b) = -0.^\circ05, -0.^\circ05$ and a boomerang-shaped arc feature which extends some 0.°25 perpendicular to, and mainly below the galactic equator at $l \simeq 0.^\circ2$. The portion of the radio continuum arc extending below the equator is the *spur*; it is connected to Sgr A at its northern tip by a *bridge* of emission which is oriented North-South in celestial (rather than galactic) coordinates. Because the overall continuum emission seen within 0.°5–1.°0 of the galactic nucleus follows the galactic equator very closely, the perpendicular orientation of the two portions of the arc is extra-ordinary.

To illustrate this behaviour, and to show why it is useful to consider the arc as consisting of the bridge and spur, we show in Fig. 1a a representation of the 10.7 GHz radio continuum map of Pauls et al. (1976; our version is from Downes et al., 1978). On the radio map we have superposed contours of the 125 μm emission mapped by Dent et al. (1982). Comparison of the two emission distributions immediately demonstrates a natural segregation of the radio structure into two parts. Of the arc, only the bridge appears at 125 μm and its mis-alignment with the galactic equator is especially apparent at that wavelength. The impression given by the Figure is that the radio bridge is composed largely of thermally-emitting material while the structure seen perpendicular to the galactic equator, the spur, is more nearly non-thermal in origin. This impression is strengthened by noting that radio recombination lines are found *only* within the infrared contours (see the maps of Güsten and Downes, 1980, and of Pauls et al., 1976).

Should the arc then be considered as a coincidental superposition of the spur and bridge features? In spite of their clear differences, the apparent coherence of the arc components nonetheless argues strongly in favour of a common origin. One factor linking the bridge and the spur is the disposition of neutral material seen near the galactic nucleus; the peculiar elongation and misalignment of the arc can be understood with reference to a single molecular cloud. Shown in Fig. 1b are the 10.7 GHz continuum map and contours of CO intensity integrated over the velocity range 40–60 km s^{-1} (from our 2.6 mm survey with 2′ spacing, Burton and Liszt, 1983). The tendency for the continuum to follow the outer boundary of the molecular material is obvious, and furthermore there are several instances of small-scale anti-correlation between the two gas species, especially just inside the spur. Sgr A itself appears at the low-longitude cloud edge, slightly offset from a peak in the molecular emission. Shaded dots in the Figure (at $\Delta l = +2'$, $\Delta b = -2'$) represent the cluster of sources discovered by Ekers et al. (1983), and are coincident with that peak.

The situation illustrated in Fig. 1b is unique in the Galaxy, for in no other instance can a neutral gas cloud be traced so clearly and so completely in the continuum. This is also apparent if one compares the continuum with the distribution of other molecules e.g. HCN (Fukui et al., 1977), and H_2CO, and NH_3 (Güsten and Henkel, 1983). And, although associations between thermally-emitting ionized material and molecular clouds are relatively commonly observed, as here on a small scale very close to Sgr A

Send offprint requests to: W.B. Burton

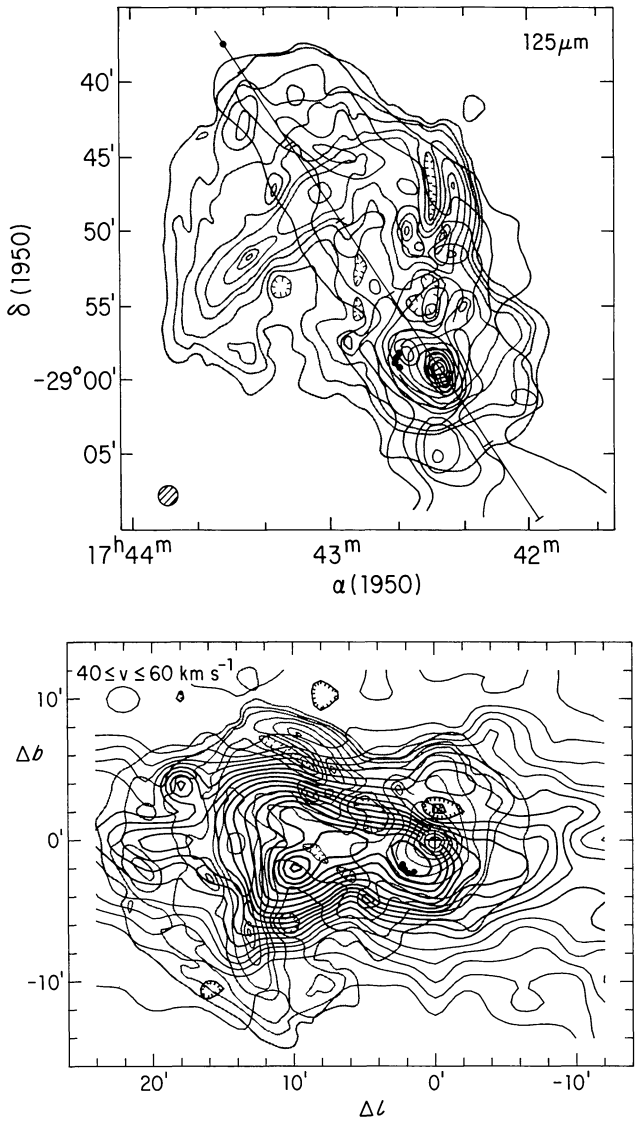

Fig. 1. a Comparison of the 125 μm infrared and 2.8 cm radio continuum distributions. Bold lines are the IR contours of Dent et al. (1982), grey shaded lines are contours of 2.8 cm continuum flux from Downes et al. (1978), and grey shaded dots represent the cluster of sources recently discovered by Ekers et al. (1983). The portions of the radio continuum overlain by IR emission constitute the bridge discussed in Sect. 1.1 and are the regions over which radio recombination lines may be detected. The regions not exhibiting IR emission, extended perpendicular to the galactic equator, comprise the non-thermal spur. **b** Comparison of the larger-scale radio continuum morphology and the disposition of the 50 km s^{-1} cloud. Here the map coordinates are galactic, taken relative to the position of Sgr A* and the heavy lines are contours of integrated radiation temperature (T_R^*/0.65) in ^{12}CO taken on a 2′ grid with a 1′ beam; contour levels are 40, 60, ... 100, 130, ... 280, 320, ... 560 K km s^{-1}

(see also Sect. 2a), clear relationships between intense CO emission and non-thermal material (as at the positive-longitude boundary of the molecular gas) are not. The observations are all the more unusual because so much of the continuum is either non-thermal or not obviously thermal.

The structure of the continuum suggests that it originates in a shell or cocoon around the neutral cloud; the spur appears perpendicular to the galactic equator because the molecular cloud has an abrupt positive-longitude boundary which is not apparent in emission or absorption studies of other species. Presumably, the molecular gas could be immersed in a flow of partially ionized material and be moving with respect to its surroundings, sweeping up ambient gas and magnetic flux. The observations now available do not determine whether the continuum structure results from external influences acting on the cloud, or whether the cloud has managed to impose itself on a pre-existing situation in such a way as to create the observed behaviour.

In several regards, the 50 km s^{-1} cloud is not an entirely unusual object. Neither its mass, $\geqq 1\ 10^6 M_\odot$, nor its size, some 40 pc, nor its well-defined edges are unusual for molecular clouds observed in the galactic disk (Liszt et al., 1981; Solomon and Sanders, 1980). It is, however, generally very intense in emission; unlike most molecular clouds in the galactic disk, it is apparently associated with a region of star formation. It also has a very large velocity dispersion. This is a characteristic which generally holds for emission and for absorption lines associated with the nucleus. It is a characteristic which distinguishes the galactic center spectra from those of the galaxy-at-large.

1.2. Kinematics of the 50 km s^{-1} cloud

The presence of gas at 50 km s^{-1} toward Sgr A indicates a substantial component of non-circular motion (assuming, of course, that Sgr A is at the galactic center and that it has no appreciable net motion with respect to the Local Standard of Rest). At the higher-longitude cloud boundary ($l \simeq 0.^\circ 2$) 50 km s^{-1} is a velocity far too small to be associated with equilibrium rotation at small galactocentric distance. The kinematic details of the 50 km s^{-1} cloud are anomalous, as is its overall velocity width. Nonetheless, these characteristics do not remain so puzzling when viewed in a larger context which we discuss in what follows.

Longitude-velocity maps of the two main CO isotopes taken near the galactic equator (Liszt and Burton, 1978; Burton and Liszt, 1980) show the following characteristics for the more widely distributed gas which *does* have a large velocity gradient around Sgr A: 1) its crossing of zero-velocity occurs at longitudes below that of Sgr A, so that there is a $\simeq$30 km s^{-1} velocity toward the galactic nucleus; 2) the velocity change with position ceases abruptly at small positive longitudes, so that there is no very high-positive-velocity gas observed at the high-longitude cloud edge. The point here is that only a very small part of the velocity of the 50 km s^{-1} cloud is obviously attributable to random motion with respect to its surroundings. This cloud is not simply plunging across the galactic nucleus and through other, more well-behaved gas.

The mean velocity of gas observed around Sgr A is strongly dependent on both latitude and longitude as can be seen in Fig. 2, a map of the intensity-weighted mean velocity of CO over the inner 200 pc constructed with data from Burton and Liszt (1983). Because features are present over a very wide range of velocity and true galactocentric distance at any position, construction and interpretation of such a diagram are not necessarily straightforward: this diagram must be understood as representing the behaviour of the more strongly-emitting gas, neglecting for the most part the contributions of the so-called expanding features observed at +165 km s^{-1}, −135 km s^{-1} near Sgr A. Comparison of the figure with position-velocity diagrams in the three immediately-preceding references will show this to be the case.

As we claimed, the kinematics of the 50 km s^{-1} cloud are part of a coherent (although unusual) pattern; there is no distortion of the mean velocity field over the limited region subtended by that strong source. Even at the longitude of Sgr A, fairly high positive

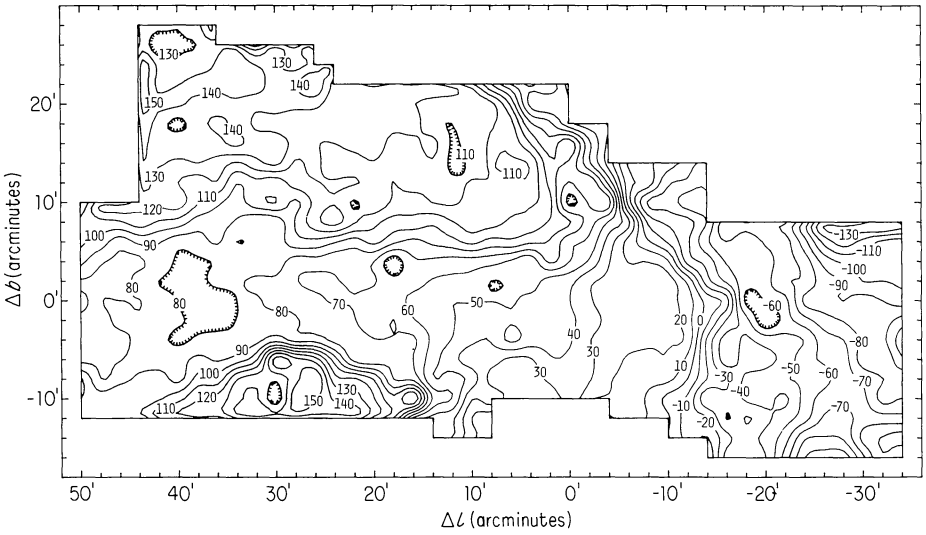

Fig. 2. Mean velocity of ^{12}CO in the Sgr A–B source complex. Note the unusual orientation of the velocity gradient across Sgr A, parallelling the 55 μm distribution and the radio bridge in Fig. 1a; it also appears in a scale of 2′ immediately around the compact source in neutral gas observed at $80 \leqq |v| \leqq 130\ \mathrm{km\,s^{-1}}$

velocities are not anomalous but the velocity gradient observed in the galactic equator at positive longitudes is quite small. Around Sgr A the most prominent velocity gradient in the sense of galactic rotation is strongly canted with respect to the galactic equator and even more strongly inclined with respect to the plane of the kpc-scale gas distribution elucidated in our original tilted models (Burton and Liszt, 1978; Liszt and Burton, 1978). This unusual orientation, which is nearly North-South in celestial coordinates and therefore similar to those of the continuum emission bridge and IR distribution, will be encountered again in the kinematics of gas observed around the non-thermal VLBI source in Sgr A (West) (Sgr A*) on a scale of only a few pc.

We cannot provide a satisfactory explanation of the gas distribution contributing to Fig. 2 which, as the more complete maps of Burton and Liszt (1983) show, is obviously very complicated. We do point out, however, that the orientation of the velocity contours is *not* due to an entirely separate gas component having the same unusual elongation. The velocities in Fig. 2 are consistent with those measured locally in H_2CO and NH_3 by Güsten and Henkel (1983, cf. their Fig. 5). Gas which appears at positive longitudes and (too-low) positive velocities near the galactic equator can be traced continuously to higher latitudes and velocities, restoring much of the kinematic symmetry which is missing in l, v maps made near the equator. Thus it is the *field* of rotational velocities as a whole which is distorted: the small velocity gradient in the galactic plane results from the fact that the true circulation axis of the gas is not normal to the galactic equator. Near zero longitude there is a component of emission, associated with the strong velocity gradient, which occurs somewhat above Sgr A at a velocity $+80\ \mathrm{km\,s^{-1}}$ (see Fig. 2 of Liszt and Burton, 1978). Thus the velocity of the $50\ \mathrm{km\,s^{-1}}$ cloud, while anomalously large in one sense, is actually negative with respect to a prominent feature at the longitude of Sgr A.

2. Smaller-scale structure

2.1. The 50 km s^{-1} cloud, near Sgr A (East)

The source Sgr A lies at the low-longitude border of the 40–$60\ \mathrm{km\,s^{-1}}$ gas and peak in the CO line temperature occurs just outside the non-thermal source previously known as Sgr A (East) (Downes and Martin, 1971; for the CO, see Liszt et al., 1975). The temperatures encountered in the carbon monoxide, greatly exceeding 10 K, are typical of those seen near giant H II regions such as Orion A, M17, and W51, but are anomalously large otherwise.

Shown in Fig. 3 is a smaller-scale version of Fig. 1b, with the 6 cm VLA continuum distribution of Ekers et al. (1983) superposed on a map of ^{12}CO emission from the 45″ beam-spacing data of Liszt et al. (1983). With the higher resolution afforded by VLA observations, the non-thermal source called Sgr A (East) by Downes and Martin (1971) is seen to be part of a full shell structure. This shell also passes through the position of the thermal emission regions at the western side of Sgr A, Sgr A (West), which is composed of a compact source (Balick and Brown, 1974), a spiral pattern of thermal emission seen at radio and near-IR wavelengths (Brown et al., 1981; Rieke et al., 1978), and some weaker, extended emission components (Brown and Johnston, 1983). The clustered sources described by Ekers et al. (1983), which are most likely compact H II regions, are coincident with the CO peak and with a feature in the 125 μm map of Dent et al. (1982). Their presence provides a rationale for the great intensity of the molecular emission at this end of the cloud: the even more intense peak at the opposite cloud edge nearest the spur is not obviously associated with any known thermal source and remains an anomaly.

The front vs. back positioning of the $50\ \mathrm{km\,s^{-1}}$ molecular gas with respect to Sgr A has been a source of continuing controversy, as has the physical disposition of the various components of the Sgr A source: much of this controversy has arisen in the context of interpretation of interferometric absorption results. The formaldehyde observations of Whiteoak et al. (1974) established that the Sgr A (East) source is strongly absorbed at $50\ \mathrm{km\,s^{-1}}$, and that the optical depth decreases substantially (to zero in their work) toward Sgr A (West); this behaviour is also present in lower-resolution synthesis of H I (Schwarz et al., 1982). Their interpretation of this situation was that the non-thermal source, not then known to be a full shell, lay behind of both Sgr A (West) and the $50\ \mathrm{km\,s^{-1}}$ cloud; the latter passed between the (East) and (West) regions. Placement of (East) behind the thermal emission regions and/or the compact source allowed an interpretation of the positive velocity in terms of ejection (see Oort, 1977), but this picture is less attractive now that (East) is known to be part of a larger source and the $50\ \mathrm{km\,s^{-1}}$ cloud has been more fully mapped.

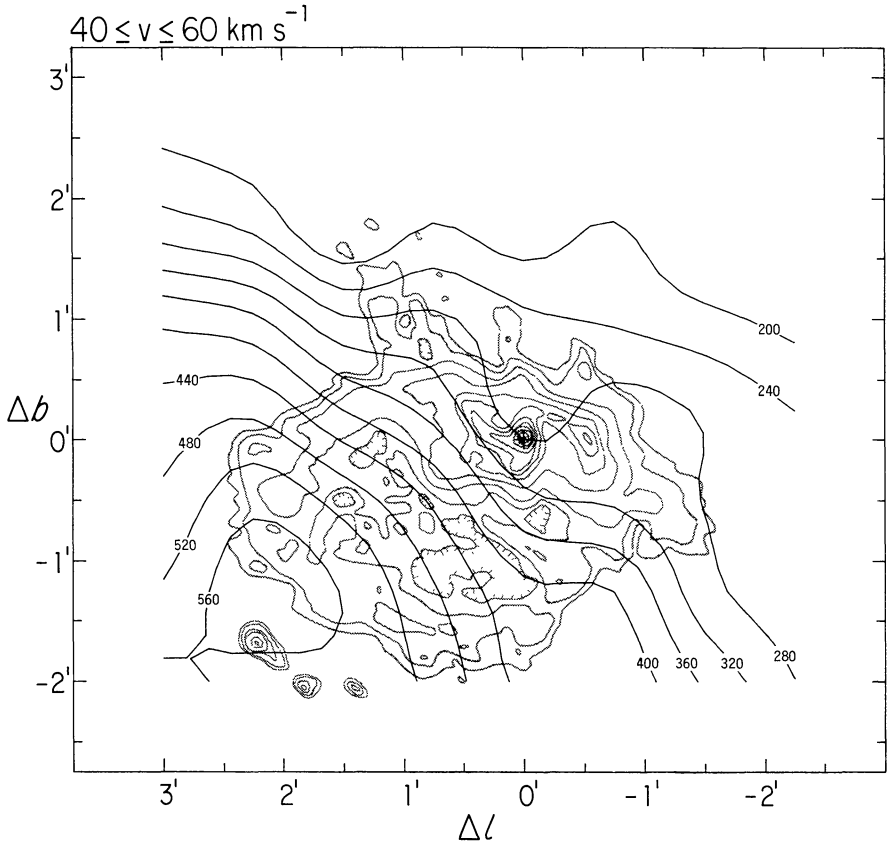

Fig. 3. Comparison of the small-scale radio continuum morphology and the disposition of the 50 km s^{-1} cloud. ^{12}CO observations (bold contours) were taken on a 45″ grid (see Liszt et al., 1983). Shaded contours represent the 6 cm flux distribution mapped by Ekers et al. (1983) at the VLA with resolution 5″ × 8″. Note the coincidence of the cluster of sources just outside the non-thermal shell with the molecular emission peak. Also note the strong gradient in emission line strength across the continuum source

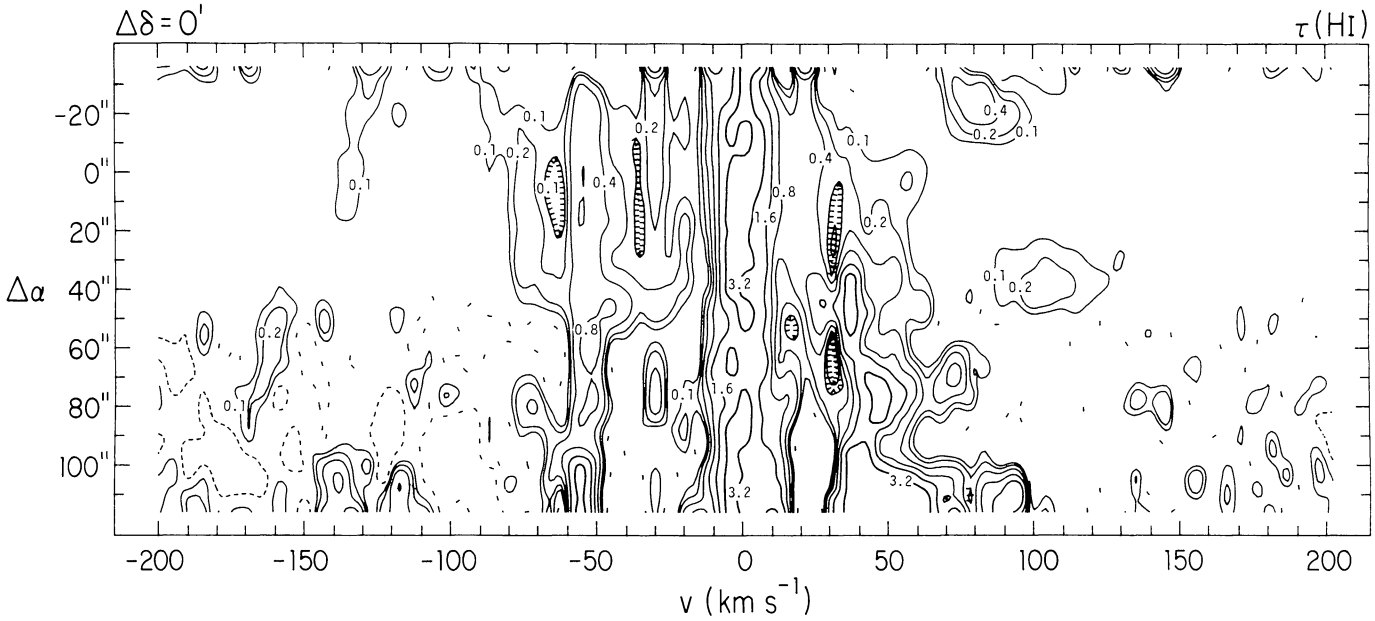

Fig. 4. Right ascension-velocity diagram of H I opacity, made at the declination of the compact source in Sgr A (which appears at $\Delta\alpha = 0''$). The H I data are from Liszt et al. (1983) and have 12″ and 6.2 km s^{-1} resolution. The spatial track of this map moves from lower left to upper right in Fig. 3. The H I absorption at 40–60 km s^{-1} decreases strongly across the continuum, as does the molecular emission, but is still visible around the compact source. The non-thermal shell Sgr A (East) is crossed some 110″ from the map origin and near Sgr A*

Measurements of molecular emission species show, as in Fig. 3, that there is a large gradient in column density across Sgr A, and Liszt et al. (1975) suggested that the observed changes in optical depth were effects of column density variations, not artifacts of geometry.

The most recent absorption-line observations, done with the VLA, can probably help settle this controversy. Shown in Fig. 4 is a right-ascension, velocity map of the H I optical depth across Sgr A, at the declination of the compact source, made from the data of Liszt et al. (1983) with 12″ spatial and 6.2 km s^{-1} velocity

resolution. The spatial track of this map, which moves diagonally from lower left to upper right in Fig. 3, crosses the non-thermal shell twice; toward Sgr A (East) at $\Delta\alpha = 110''$, and toward Sgr A (West) around $\Delta\alpha = 0''$. The absorption line strength at 40–60 km s^{-1} decreases as the position of Sgr A* is approached from the East but does not vanish there. Because of this behaviour, and because a higher-resolution spectrum also found an opacity of $\simeq 0.25$, Liszt et al. (1983) concluded that both the thermal emission regions and the compact source in Sgr A lay behind the 50 km s^{-1} cloud.

This change in opacity from (East) to (West) could be an artefact in the VLA observations *only* if the absorbing gas in front of (East) has a much smaller scale structure than the absorbed continuum. In such a situation the insensitivity of the VLA observations to large scale structure in the continuum could artificially enhance the optical depth $\tau (= T_L/T_C)$ at (East). We think this is not the case, also in view of the very similar results of Schwarz et al. (1982), whose observations are not insensitive to the larger scale structure in (East).

In the companion paper (Liszt et al., 1984) we showed that the 40–60 km s^{-1} H I absorption toward Sgr A* persists at $\tau \simeq 0.25$ with 1.″5 resolution, and we discussed ways in which our H I measurements could be reconciled with the H_2CO synthesis of Whiteoak et al. (1983). With a spatial resolution of 3.″5 at 6 cm, the molecular gas is present toward portions[1] of the thermal spiral around Sgr A* but not toward it. A small gap in the intervening gas, combined with the $\simeq 130$ times larger solid angle of the compact source at 21 cm, will accomodate the observations, but there are other interpretations. More relevant here is the question of the cause of the absorption. According to discussion up to this point, using Figs. 3 and 4, it would appear to be the edge of the 50 km s^{-1} cloud, but this is not the case.

2.2. *The ring around Sgr A**

If the 40–60 km s^{-1} absorption observed over Sgr A (West) were due to the 50 km s^{-1} cloud, a map similar to Fig. 4 but moving in declination through Sgr A* would be expected to show the absorption rather ubiquitously: a portion of the 21-cm continuum flux along such a line is presumably due to the shell. If the shell structure were uniformly strongly absorbed [as toward Sgr A (East)] the 40–60 km s^{-1} feature would be very strong indeed, independent of the relative positioning of Sgr A (West) and the molecular cloud.

A declination-velocity map of the H I absorption is shown in Fig. 5. The track of this map is diagonal from lower right to upper left in Fig. 3, and is about parallel to the 125 μm distribution in Fig. 1a (i.e., parallel to the radio bridge), or to the velocity gradient around Sgr A in Fig. 2. Along this line the 40–60 km s^{-1} gas is confined and clearly separate from lower-velocity absorption. The behaviour of the 40–60 km s^{-1} absorption in this map indicates that the non-thermal shell is at most very weakly absorbed near its western boundary. The column density effects expected from the CO map must actually cause the steep east-west differences in opacity which were previously used to infer that Sgr A (East) lay behind (West), with the 50 km s^{-1} cloud passing in-between (Whiteoak et al., 1974).

Along the spatial track of Fig. 5 the 40–60 km s^{-1} absorption around Sgr A* has a large velocity gradient, of order 100 km s^{-1} arcmin^{-1}, which is most certainly *not* a property of the 50 km s^{-1} cloud. Also present in Fig. 5 (but not visible along the orthogonal track in Fig. 4) are high positive- and negative-velocity gas components ($|v| \geqq 80$ km s^{-1}) showing a fair degree of symmetry about the map origin. These structures are visible in the CO (Fig. 6) as twin lobes and must arise from density enhancements. The general impression given by Figs. 4–6 is of a ring of material rotating about an axis passing through or very near Sgr A*, seen close to edge-on. Figure 4, which shows no velocity gradient in the 40–60 km s^{-1} gas and no high $-|v|$ absorption must be nearly parallel to the rotation axis, while the track of Fig. 5 follows the approximate major axis of the gas ring. The behaviour of the 40–60 km s^{-1} gas in that Figure indicates a substantial inward-directed component of motion of the ring material. The dashed lines in Fig. 5 arise from a model of this behaviour.

The model optical depth contours have been calculated for the front side [neglecting absorption arising from gas more distant than the plane 10 kpc $(\cos(l)\cos(b))^{-1}$] of a thick ring which makes an angle of 20° with respect to the line of sight. The ring density is Gaussian about the mean radius 3.2 pc halfwidth 0.6 pc, and Gaussian about the mean plane with halfwidth 0.9 pc. The velocity of rotation is 110 km s^{-1} and the velocity of infall is 52 km s^{-1}; the internal gas dispersion is 10 km s^{-1} and the model contours have been convolved with a 12″ Gaussian beam. As expected, the apparent kinematics of the model reproduce the observed behaviour. The model predicts too large an optical depth on one side of the source, but is rather successful in reproducing the profile shapes. Apparently, it can not be concluded that the 40–60 km s^{-1} gas absorbing Sgr A (West) is the same as that seen more strongly against Sgr A (East).

The velocity of rotation in the model is about the same as that seen in ionized gas at the ends of the thermal emission spiral (van Gorkom et al., 1984; see also Oort, 1984; and Lo and Claussen, 1983). The ring is about twice as large as the thermal spiral, however, and the interior mass calculated on assumption of centrifugal equilibrium is 8 $10^6 M_\odot$. (Of course there is no reason to believe that such equilibrium applies.) We caution the reader that the kinematics of a circular gas pattern having superposed rotational and radial motions can be reproduced as well by circulation along elliptical paths (compare the discussion in Burton and Liszt, 1978, and Liszt and Burton, 1980). Although the infall model employed here has the virtue of simplicity, it cannot be proved that the gas around Sgr A is falling into the galactic nucleus in a bulk manner.

The mass of H I in the model illustrated is 5 $M_\odot$ if the H I spin temperature is 15 K and the absorption arises from a residual atomic gas fraction in predominantly molecular material (see Liszt et al., 1983); this is probably a lower limit. The mass of molecular material is much larger, but very uncertain. There could be as much as several hundred star masses of molecular material in the ring and it seems likely that the mass of neutral molecular material in the ring exceeds that of the thermal ionized gas around Sgr A, which Ekers et al. (1983) estimate at a few dozen $M_\odot$.

2.3. *Geometry of the material seen around Sgr A**

Double-lobed structure around Sgr A occurs on a smaller scale in the infrared emission maps of Becklin et al. (1982): separation between the IR lobes is about one arcmin and they are seen in

1 Because so little of the continuum *is* clearly occulted in H_2CO, it seems worth noting that one prominent absorption occurs at IRS 4 near the extreme eastern edge of the thermal spiral. This low-contrast, extended IR source has been shown by Willner and Pipher (1982) to possess a 3.3 μm emission feature characteristic of the interface between H II regions and molecular material

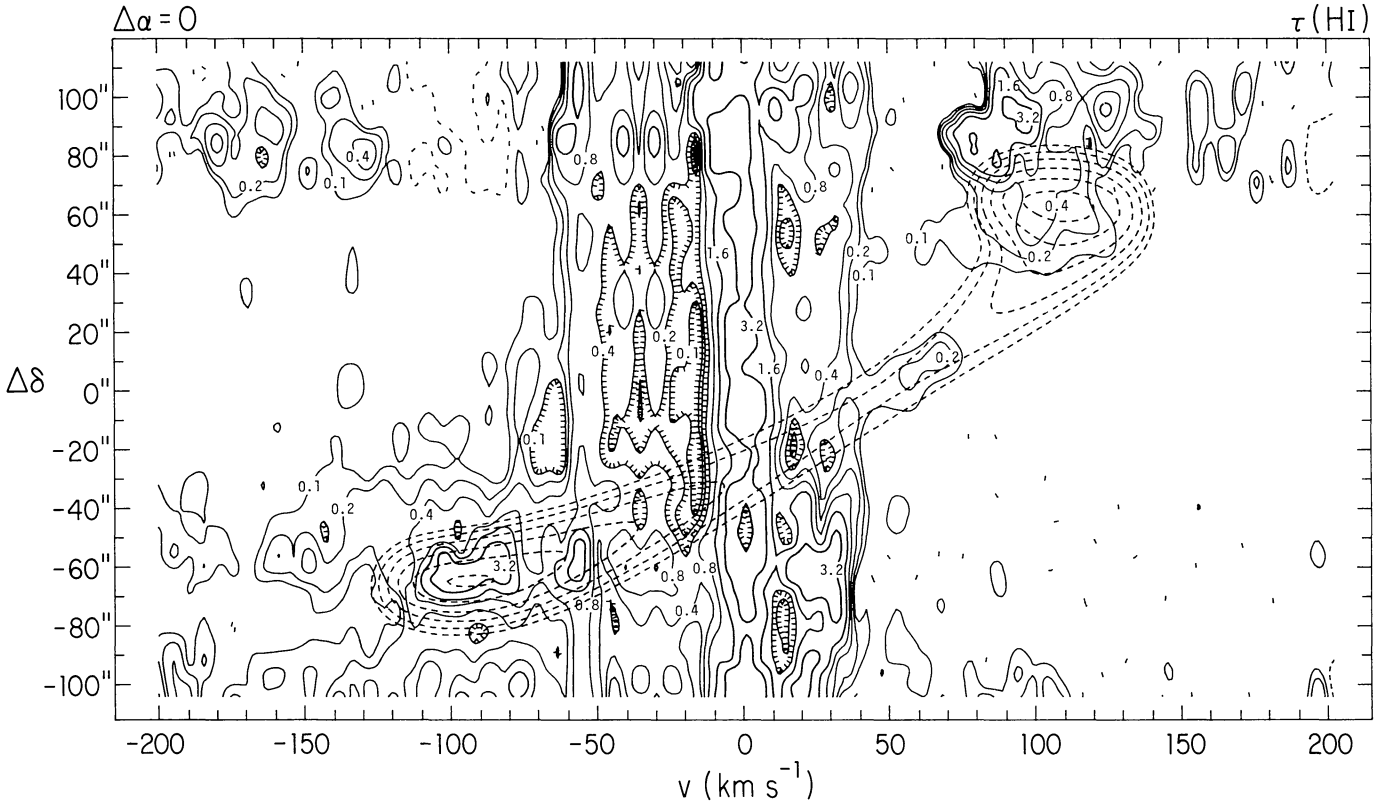

Fig. 5. Declination-velocity diagram of H I opacity through the compact source position. In these coordinates absorption at velocities 40–60 km s^{-1} appears quite separate and has an appreciable velocity gradient. Higher-velocity absorption ($80 \leqq |v| \leqq 130$ km s^{-1}) appears rather symmetrically about the map origin. Dashed contours are for a ring model discussed in Sect. 2.2 of the text; the ring has mean radius 3.2 pc (65″), position angle 0°, and inclination 70°. It is rotating at 110 km s^{-1} and infalling at $\simeq$ 50 km s^{-1}. The ring major axis, which lies along the spatial track of this diagram, is parallel to the unusual orientation of the larger-scale velocity gradient (and other structure) noted in Fig. 2 (Sect. 1.1 of the text)

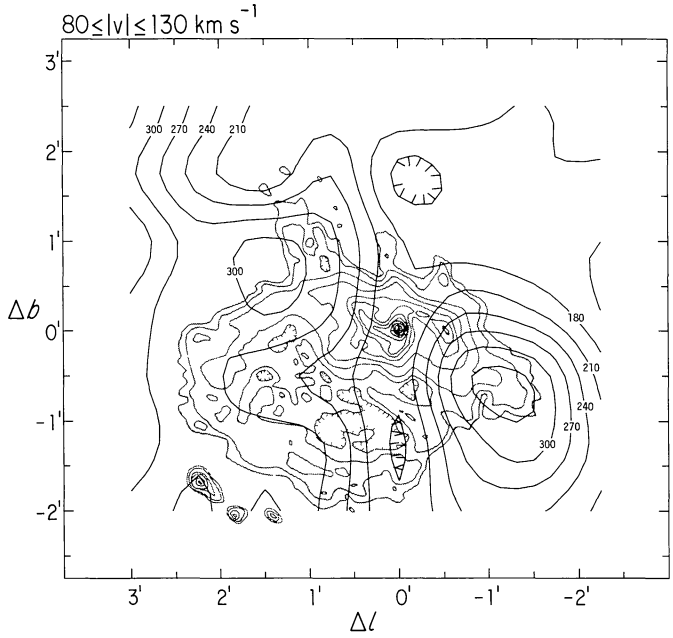

Fig. 6. As in Fig. 3, but the range of integration for the ^{12}CO intensity is $80 \leqq |v| \leqq 130$ km s^{-1}. The ends of the ring appear in emission, indicating that the gas column density (not merely the apparent optical depth in H I) is actually larger there

projection against the ends of the North and South arms of the thermal emission spiral. Their orientation is only slightly displaced from a line of constant galactic latitude, but in the sense of our ring. Spectra taken of the 63 μm O I fine-structure yields velocities ± 80 km s^{-1} for the IR lobes, in the sense of galactic rotation (Genzel, private communication); analysis of the O I lines yields densities comparable to those we infer from the H I and CO column densities (Genzel et al., 1982, 1983). Although the O I spatial distribution actually appears to be centrally peaked, this is almost certainly an artifact of the $\simeq$40″ resolution employed: no other species associated with the neutral gas, atomic or molecular, shows a centrally-peaked distribution (see also Fukui et al., 1982).

The infrared structure probably arises at the heated inner edge of the neutral gas mapped in H I and CO. At still smaller distances from Sgr A*, $\leqq$1 pc, the 30–100 μm maps of Becklin et al. (1982), combined with the similarity of the distribution of the radiation at 10.6 μm and 6 cm (Rieke et al., 1978; Brown et al., 1981; Lo and Claussen, 1983), indicate that the gas is ionized (see Brown and Liszt, 1984). Thus, fitting the H I–CO gas ring neatly around the Sgr A continuum (which is implied by our modelling in Fig. 5) is not a problem; the ring discussed here can naturally be grafted onto the previously existing observations to yield a coherent picture in which gas at progressively larger distances from the galactic nucleus is first ionized, then warm and neutral, then cool and neutral. The H I ring is the warm, neutral transition region between the hot, ionized inner parts and the cold, molecular outer

parts of an extended gas distribution. Much of the continuum being absorbed by the H I arises from the inner regions of the same structure.

Elucidation of the ring structure, which clarifies the situation vis-à-vis the 40–60 $km s^{-1}$ absorption around Sgr A*, does not, however, directly address the positioning of Sgr A or its various parts with respect to each other and to the 50 $km s^{-1}$ cloud. The H I position-velocity maps (Figs. 4 and 5) indicate that the non-thermal shell is behind the (edge of the) cloud and that the east-west gradients in opacity across Sgr A result from a decline in the quantity of the occulting gas as expected from the CO emission behaviour in Figs. 1b and 3. If the larger-scale structure of the radio arc, 55 μm emission, etc., is associated with Sgr A, their striking coincidence with the boundaries of the molecular material strongly implies that all of the inner-galaxy radio continuum structure occurs near the cloud; the arc and the various parts of Sgr A must be associated with each other as well as with the molecular cloud. Thus we suggest that the 50 $km s^{-1}$ cloud exists close to the nucleus, that the non-thermal shell resides only slightly behind the molecular material, and that the compact sources observed just outside the shell are very close to or embedded within the molecular cloud; the presence of H II regions and a possible supernova remnant near a molecular cloud is hardly astonishing. Sgr A (West), Sgr A*, and the H I ring, all of which are intimately related, are also near the cloud and the shell.

The most problematical aspect of reconstructing the geometry remains the positioning of the shell with respect to Sgr A (West), i.e. to Sgr A* and its surrounding gas ring. The shell and the rest of Sgr A must be fairly close to each other, but we have no way of knowing whether the projection of the western rim of the shell against Sgr A (West) is a coincidence or if the shell material is actually sweeping across the galactic nucleus. Given the well defined edge of the 50 $km s^{-1}$ cloud and the fact that the 40–60 $km s^{-1}$ absorption toward Sgr A (West) arises from the ring, the ability of the absorption measurements to determine the inner-galaxy geometry is seriously, probably fatally, compromised. The edge of the 50 $km s^{-1}$ cloud seen toward Sgr A could be so sharp that there is really no neutral material left to interpose between the shell and Sgr A (West). Whatever the case, this aspect of the inner-galaxy geometry is probably a minor detail, not a major determinant of the inferred behaviour.

3. Summary

a) The larger-scale continuum distribution about Sgr A is distributed around the 40–60 $km s^{-1}$ molecular cloud. It is seen projected against the neutral cloud boundary over that boundary's nearly full extent. In discussing how that situation might arise, we showed that the velocity of the molecular material fits well into the larger-scale kinematics observed in the inner few hundred pc of the Galaxy; it is not a random motion. Contours of the mean velocity of the molecular material have several unusual properties, one of which is that the apparent axis of rotation of the strongly emitting ^{12}CO seen around Sgr A is clearly not normal to the galactic equator. This peculiarly-oriented axis also appears in the infrared and radio continuum structure on a scale of 50 pc, and very close to Sgr A*.

b) The Sgr A source lies at the low-longitude boundary of the 50 $km s^{-1}$ cloud, just outside a strong peak in the molecular emission intensity. The eastern edge of the non-thermal shell in Sgr A abuts this peak; coincident with the peak as we see it is a newly-discovered cluster of H II regions which is probably responsible for heating of the molecular gas.

c) There is a ring of mean radius 3.2 pc rotating about Sgr A* with velocity $\simeq 110 km s^{-1}$. It appears in both ^{12}CO emission and H I absorption and is seen sufficiently edge-on (20° from the line-of-sight) that it appears as two lobes. The conventional position angle of the ring, 0° in celestial coordinates, is such that its apparent rotation axis mimics the unusual orientation of the larger-scale material cited in the first part of this summary. This neutral gas ring is the outer portion of the same body giving rise to a similar but smaller (1.5 pc) twin-lobe pattern at 30–100 μm in the infrared.

d) The kinematics of the 40–60 $km s^{-1}$ gas seen in absorption toward the inner parts of Sgr A (West) indicate that the ring has a $\simeq 50 km s^{-1}$ component of inward-directed motion which is most simply modelled as infall but which could undoubtedly also be reproduced by a pattern of circulation along elliptical orbits. The 40–60 $km s^{-1}$ absorption observed over Sgr A (West) arises in the ring, not in the 50 $km s^{-1}$ cloud which absorbs more strongly to the east.

e) The presence of an additional component of positive velocity gas (the ring) and the projection of Sgr A against the edge of the 50 $km s^{-1}$ cloud complicate reconstruction of the continuum geometry through the use of absorption spectra only. Nonetheless, our H I absorption results suggest that the east-west decline in opacity across Sgr A at 40–60 $km s^{-1}$ is due to a decrease in the column density of the 50 $km s^{-1}$ molecular cloud (not to passage of the cloud between Sgr A East and West). The edge of the cloud seen in the vicinity of Sgr A is probably sharp enough that there is little material to interpose between the non-thermal shell and Sgr A (West) even if one does lie slightly closer than the other. The sum of the observations discussed here suggests that *all* the various parts of Sgr A are associated with each other and with the 50 $km s^{-1}$ cloud.

A wide variety of observations, now in progress, should elucidate the conditions shaping the gaseous morphology of the innermost regions of the Galaxy. Yusef-Zadeh et al. (1984) have mapped the continuum distribution on the scale shown in Fig. 1, using the VLA in several configurations, and have discovered a variety of substructures not previously accessible. Molecular emission observations can now be undertaken with beam areas at least an order of magnitude smaller than that available to us in ^{12}CO; structure near Sgr A and at the apparent interface between the continuum arc and the 50 $km s^{-1}$ cloud will be mapped in vastly greater detail. The results presented here indicate that ionized and neutral gas are intimately related on many scales observed in and around the Sgr A source complex; the distribution of one cannot be understood fully without reference to the other.

Acknowledgements. WBB and HSL gratefully acknowledge support for this work from the North Atlantic Treaty Organization Grant No. 008.82. The National Radio Astronomy Observatory is operated by Associated Universities, Inc. under contract with the National Science Foundation. The Netherlands Foundation for Radio Astronomy (S.R.Z.M.) is supported by the Netherlands Organization for the Advancement of Pure Research (Z.W.O.).

References

Balick, B., Brown, R.L.: 1974, *Astrophys. J.* **194,** 265
Becklin, E.E., Gatley, I., Werner, M.W.: 1982, *Astrophys. J.* **258,** 135
Brown, R.L., Johnston, K.J., Lo, K.Y.: 1981, *Astrophys. J.* **250,** 155
Brown, R.L., Johnston, K.J.: 1983, *Astrophys. J. Letters* **268,** L85

Brown, R.L., Liszt, H.S.: 1984, *Ann. Rev. Astron. Astrophys.* **22** (in press)
Burton, W.B., Liszt, H.S.: 1978, *Astrophys. J.* **255,** 815
Burton, W.B., Liszt, H.S.: 1980, in *Origin of Cosmic Rays*, eds. G. Setti, G. Spada, A.W. Wolfendale, D. Reidel, Dordrecht, p. 227
Burton, W.B., Liszt, H.S.: 1983, in *Surveys of the Southern Galaxy*, eds. W.B. Burton, F.P. Israel, D. Reidel, Dordrecht, p. 149
Dent, W.A., Werner, M.W., Gatley, I., Becklin, E.E., Hildebrand, R.H., Keene, J., Whitcomb, S.E.: 1982, in *The Galactic Center*, eds. G.R. Riegler, R.D. Blandford, AIP, New York, p. 33
Downes, D., Goss, W.M., Schwarz, U.J., Wouterloot, J.G.A.: 1978, *Astron. Astrophys. Suppl.* **35,** 1
Downes, D., Martin, A.H.M.: 1971, *Nature* **233,** 112
Downes, D., Maxwell, A.: 1966, *Astrophys. J.* **146,** 653
Ekers, R.D., van Gorkom, J.H., Schwarz, U.J., Goss, W.M.: 1983, *Astron. Astrophys.* **122,** 143
Fukui, Y., Iguehi, T., Kaifu, N., Chicada, Y., Morimoto, M., Nagane, K., Miyazawa, K., Miyaji, T.: 1977, *Publ. Astron. Soc. Japan* **29,** 643
Fukui, Y., Ogawa, H., Deguchi, S., Suzuki, H.: 1982, in *The Galactic Center*, eds. G.R. Riegler, R.D. Blandford, AIP, New York, p. 18
Gatley, I.: 1982, in *The Galactic Center*, eds. G.R. Riegler, R.D. Blandford, AIP, New York, p. 25
Genzel, R., Watson, D., Townes, C., Lester, D., Dinerstein, H., Werner, M., Storey, J.: 1982, in *Galactic Center*, eds. G.R. Riegler, R.D. Blandford, AIP, New York, p. 72
Genzel, R., Watson, D.H., Townes, C.H., Dinerstein, H.L., Hollenbach, D., Lester, D.F., Werner, M., Storey, J.W.V.: 1983 (preprint)
van Gorkom, J.H., Schwarz, U.J., Bregman, J.: 1984 (in preparation)
Güsten, R., Downes, D.: 1980, *Astron. Astrophys.* **87,** 6
Güsten, R., Henkel, C.: 1983, *Astron. Astrophys.* **125,** 136
Liszt, H.S., Burton, W.B.: 1978, *Astrophys. J.* **226,** 790
Liszt, H.S., Burton, W.B.: 1980, *Astrophys. J.* **236,** 779
Liszt, H.S., Burton, W.B., van der Hulst, J.M.: 1985, *Astron. Astrophys.* **142,** 245
Liszt, H.S., van der Hulst, J.M., Burton, W.B., Ondrechen, M.: 1983, *Astron Astrophys.* **126,** 341
Liszt, H.S., Sanders, R.H., Burton, W.B.: 1975, *Astrophys. J.* **198,** 537
Liszt, H.S., Xiang, D., Burton, W.B.: 1981, *Astrophys. J.* **249,** 532
Lo, K.Y., Claussen, M.J.: 1983, *Nature* **306,** 647
Oort, J.H.: 1977, *Ann. Rev. Astron. Astrophys.* **15,** 295
Oort, J.H.: 1984, in *The Milky Way Galaxy*, eds. H. van Woerden, W.B. Burton, R. Allen, Reidel, Dordrecht (in press)
Pauls, T., Downes, D., Mezger, P.G.: 1976, *Astron. Astrophys.* **46,** 407
Rieke, G.H., Telesco, C.M., Harper, D.A.: 1978, *Astrophys. J.* **220,** 149
Schwarz, U.J., Ekers, R.D., Goss, W.M.: 1982, *Astron. Astrophys.* **110,** 100
Solomon, P.M., Sanders, D.B.: 1980, in *Giant Molecular Clouds in the Galaxy*, eds. P.M. Solomon, M.G. Edmunds, Pergamon, New York, p. 41
Whiteoak, J.B., Gardner, F.F., Pankonin, V.: 1983, *Monthly Notices Roy. Astron. Soc.* **202,** 11p
Whiteoak, J.B., Rogstad, D.H., Lockhart, I.A.: 1974, *Astron. Astrophys.* **33,** 413
Willner, S.P., Pipher, J.L.: 1982, in *The Galactic Center*, eds. G.R. Riegler, R.D. Blandford, AIP, New York, p. 77
Yusef-Zadeh, F., Morris, M., Chance, D.: 1984, *Astrophys J. Letters* (submitted)